CQICO and Multi-objective Thermal Optimization for High Speed PM Generator

Xiaochen. Zhang[1,3], Weili. Li[1], Chris. Gerada[2,3], He. Zhang[2,3], Jing Li[2], Michael. Galea[2], David. Gerada[2], Junci.Cao[1]

[1]School of Electrical Engineering, Beijing Jiaotong University, Beijing, 100044, China
[2]IAMET, University of Nottingham, Ningbo, Zhejiang, 315100, China
[3] Department of Electrical and Electronic Engineering, University of Nottingham, Nottingham, NG7 2RD UK

This paper proposes a novel Continuous Quantum Immune Clonal Optimization (CQICO) algorithm for thermal optimization on an 117kW high speed permanent magnet generator (HSPMG). The proposed algorithm mixes the Quantum Computation into the Immune Cloning Algorithm and causes better population diversity, higher global searching ability, and faster convergence which approved by simulation results. Then, the improved algorithm is applied to seek an optimized slot groove and improve HSPMG thermal performance, in which the 3-D fluid-thermal coupling analyses are processed with a multi-objective optimal group composed of the highest temperature and the temperature difference. Both the proposed algorithm and the obtained conclusions are of significances in the design and optimization of the cooling system in electric machines.

Index Terms— CQICO, HSPMG, Fluid-thermal, Groove, Optimization.

I. INTRODUCTION

THE Immune Cloning Algorithm (ICA) is a kind of high-performance optimization algorithm developed from the biological Immune Clonal Selection Principle [1][2], and the quantum computation is a new method in accordance with the quantum mechanics theories [3]. At present, many researchers devoted to studying Quantum Immune Clonal Optimization algorithm research, and some have applied it to the optimization of electrical machines [4-8].

The high-speed permanent magnet generator (HSPMG) [9][10] offers high power density, small size and high efficiency for applications such as micro turbine generation system, household appliances and industrial drives. The electromagnetic loss and the mechanical loss in HSPMG increase remarkably due to the high frequency and high speed, which results in high thermal load. The working temperature is relatively higher than that of normal electrical machines, which requests a better cooling system to ensure machine durability, reliability and avoid magnet demagnetization. Moreover, the elongated structure of HSPMG increased the temperature difference in machine along the axial direction. Thus, an optimized cooling system has of important significance for HSPMG, which reduce the impacts of both high temperature and disequilibrium thermal stress.

In this paper, a novel Continuous Quantum Immune Clonal Optimization (CQICO) is proposed, and it is successfully applied to the optimization of the cooling system of a 100kW level HSPMG. Via the fluid-thermal coupling analysis, the 3-D temperature distributions are investigated. Then, stator slot groove structure is optimized by the proposed CQICO. The results from both CQICO and numerical analyses indicate the effectiveness of the new structure cooling system in improving the machine temperature distribution.

II. CONTINUOUS QUANTUM IMMUNE CLONAL OPTIMIZATION

In the proposed CQICO, each antibody is represented by a coded qubit, which distributes with a random probability. A qubit could not only express the state of 0 or 1, but also any state between them. Thus, a series of 2^n status can be expressed by qubits with amount of n. Therefore, for the same optimization problem, the population size of CQICO is much smaller than that of ICA. The probability amplitude of k qubits can be written as

$$q = \begin{bmatrix} \alpha_1 & \alpha_2 & \cdots & \alpha_k \\ \beta_1 & \beta_2 & \cdots & \beta_k \end{bmatrix}, \tag{1}$$

where, α and β are the probability amplitudes of state 0 and 1, respectively, and $|\alpha|^2 + |\beta|^2 = 1$.

By using the bit code, an initial antibody group composed of m antibodies is built, and one antibody could be

$$q_j = \begin{bmatrix} \alpha_{11} & \alpha_{12} & \cdots & \alpha_{1k} & \alpha_{21} & \alpha_{22} & \cdots & \alpha_{2k} & \cdots & \alpha_{m1} & \alpha_{m2} & \cdots & \alpha_{mk} \\ \beta_{11} & \beta_{12} & \cdots & \beta_{1k} & \beta_{21} & \beta_{22} & \cdots & \beta_{2k} & \cdots & \beta_{m1} & \beta_{m2} & \cdots & \beta_{mk} \end{bmatrix}, \tag{2}$$

where, j is the antibody number, and $1 \le j \le m$

For a qubit could possess the state of 0, 1, or both, the qubits are in high superposition states. On the other hand, the states of subsystems are not independent of each other, which means the appearance high entanglement states. So the antibody update and the high frequency mutation operations, which often used in the traditional ICA, cannot be adopted in CQICO. Here, the quantum gates are introduced to deal with the entanglement state and the superposition state, via updating or mutating the antibodies with a high frequency.

In the process, the quantum rotation gate $U(\theta)$ is used to update the qubits. $U(\theta)$ is a unitary matrix with dimensions of 2×2. If α and β are written as $\cos(\phi)$ and $\sin(\phi)$ the quantum state is changed as

$$U\begin{bmatrix}\cos(\phi)\\\sin(\phi)\end{bmatrix}=\begin{bmatrix}\cos(\theta) & -\sin(\theta)\\\sin(\theta) & \cos(\theta)\end{bmatrix}\begin{bmatrix}\cos(\phi)\\\sin(\phi)\end{bmatrix}=\begin{bmatrix}\cos(\phi+\theta)\\\sin(\phi+\theta)\end{bmatrix}, \quad (3)$$

where, ϕ is the initial qubit angle, and $0\le\phi\le2\pi, 0\le\theta\le2\pi$.

If the selected antibody is

$$P_k=\begin{vmatrix}\cos(\theta_1^k)\\\sin(\theta_1^k)\end{vmatrix}\begin{vmatrix}\cos(\theta_2^k)\\\sin(\theta_2^k)\end{vmatrix}\cdots\begin{vmatrix}\cos(\theta_r^k)\\\sin(\theta_r^k)\end{vmatrix}. \quad (4)$$

The cloned antibodies through the quantum gates would be

$$P_{ks}=\begin{vmatrix}\cos(\theta_1^k+\Delta\theta_{1s}^k)\\\sin(\theta_1^k+\Delta\theta_{1s}^k)\end{vmatrix}\begin{vmatrix}\cos(\theta_2^k+\Delta\theta_{2s}^k)\\\sin(\theta_2^k+\Delta\theta_{2s}^k)\end{vmatrix}\cdots\begin{vmatrix}\cos(\theta_r^k+\Delta\theta_{rs}^k)\\\sin(\theta_r^k+\Delta\theta_{rs}^k)\end{vmatrix}, \quad (5)$$

where, $s=1, 2, …, N_k$.

Meanwhile, the expanded population is space transformed. Antibodies with poorer affinity are selected and mutated by the quantum NOT-gate P, which could be described as (6), and the basic NOT transformations for qubits is (7).

$$P=\begin{bmatrix}0 & 1\\1 & 0\end{bmatrix} \quad (6)$$

$$P\begin{bmatrix}\alpha\\\beta\end{bmatrix}=\begin{bmatrix}0 & 1\\1 & 0\end{bmatrix}\begin{bmatrix}\alpha\\\beta\end{bmatrix}=\begin{bmatrix}\beta\\\alpha\end{bmatrix} \quad (7)$$

For CQICO within the definitional domain of the functions, an initial antibodies group P composed of m antibodies is established, which is divided into the memory cell group M and the reminder group P_r. Then, the affinity of each antibody is estimated, and the affinity of antibody i is F_i^1, and it is also divided into two parts, that is $P=P_r+M$. The antibodies with highest affinity are selected and cloned, and the new generated antibodies compose the new group P'. Whereas for the antibodies with poorer affinity, it have been mutated by using (7). Only if the affinity of antibody i is larger than that before mutation, these antibodies will be replaced by the mutated ones. Through the antibody affinity judgment, to determine whether the concentration suppressed is carry out, and then go to the next iteration calculation.

In order to test the optimized performance of CQICO, three typical functions, listed in Table. I, are simulated and analyzed. Fig. 1 shows the initial and the final antibody position distributions in the CQICO optimization on function F_1. The population size is 50 in this study. In the final position antibody distribution, Fig. 1(b), all the antibodies locate at the global maximum point, which indicates the improved global searching ability of CQICO.

TABLE I
FUNCTIONS USED IN NUMERICAL SIMULATION

	Functions	Domain
F_1	$x^3+y^3-12(x+y)$	$x、y\in[-4,4]$
F_2	$1+x\sin(4\pi x)-y\sin(4\pi y+\pi)$	$x、y\in[-1,1]$
F_3	$(3/(0.05+x^2+y^2))^2+(x^2+y^2)^2$	$x、y\in[-5.12,5.12]$
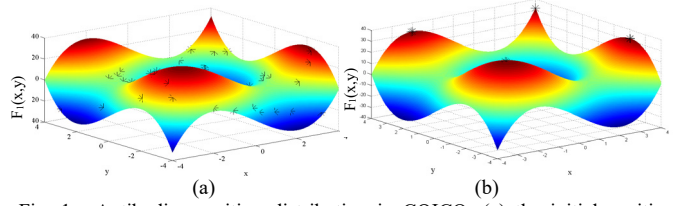
Fig. 1. Antibodies position distribution in CQICO: (a) the initial position distribution, (b) the final position distribution.
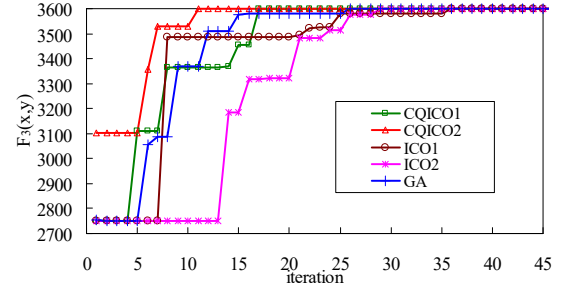
Fig. 2. Evolutionary curves of function F_3.

In order to estimate the convergence speed, the objective functions in Table. I are optimized by using the CQICO$_1$(population size 30), CQICO$_2$ (population size 50), the Immune Clonal Optimization (ICO$_1$ population size 30, ICO$_2$ population size 50,), and the Genetic Algorithm (GA), respectively. Fig 2 shows the evolutionary curves on F_3. From the figure, it can be seen that all the algorithms converge to the same solution and the CQICO has faster convergence than ICO and GA. While with the same population size, the iterations of CQICO are much less than that of the ICO. When with the same population size, the iteration time of CQICO is about 1/3 of the iteration times that ICO needed, which is averagely 32% of that GA needed. For CQICO, the iteration is faster with larger population size.

III. TEMPERATURE DISTRIBUTIONS IN HSPMG

Fig. 3 shows the prototype of HSPMG studied in this paper. The machine with a rated power of 117kW operates under the speed of 60000rpm, and the output voltage of stator windings terminal is 670V. Rotor magnets is SM-26U, with a highest working temperature of 350 ℃. The length of armature core is 275 mm, and the outer diameter of the stator and rotor are 135 mm and 66 mm, respectively. The rotor sleeve is made of 50Mn18Cr5 and with a thickness of 5.5mm.

The investigated HSPMG is cooled by an enclosed oil system, and a cylindrical epoxy resin stator sleeve is inserted in machine air-gap to keep the cooling oil sealed in stator side. Moreover, a back wound armature windings are adopted to enhance the cooling effectiveness.

A segment of the HSPMG is selected for the coupling calculation model due to the symmetrical structure and loss distribution, as shown in Fig.4. The material properties, such

Fig. 3. Prototype stator and rotor.
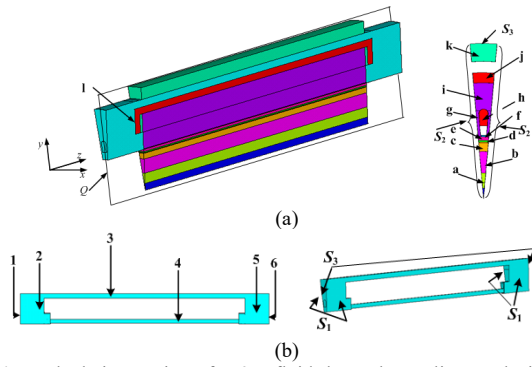
Fig. 4. Calculation regions for 3D fluid-thermal coupling analysis: (a) the solid region, (b) the fluid region.
1-fluid inlet, **2**-inlet end fluid, **3**-fluid in yoke back room, **4**-fluid in slot grooves, **5**- outlet end fluid, **6**-outlet.
a-rotor yoke, **b**-PM, **c**-sleeve, **d**-air-gap, **e**-oil separator, **f**-tooth-top, **g**-tooth, **h**-equivalent windings, **i**-yoke, **j**-back windings, **k**-frame.

as electrical conductivity and thermal conductivity are treated as variable with the working temperature, which are determined from the multi-physical fields modeling. The boundaries for such calculation are:

I. Fluid outer surfaces (S_1) be applied the thermal insulation boundary. Both the tooth and slot axial center surfaces are insulation faces (S_2) meet the adiabatic boundary.

II. The heat transferred through the interface between rotor and shaft is ignored. For the frame outer surface (S_3), it satisfies the third boundary condition.

III. For fluid inlet and outlet, the entrance(1 in Fig.4 b) is applied the mass flow condition, whereas the outlet (6 in Fig.4 b) the pressure condition is used.

The eddy current losses in the rotor sleeve are determined via transient electromagnetic field analyzing, so as the stator core loss. The friction loss on the rotor outer surface is calculated by analytical questions. Whilst, the thermal analysis models for rotating air in air-gap and stator coils are proposed [10].

The built model is fluid-thermal coupling analyzed by using Finite Volume Method. Fig.5 shows the flowing velocity in the slot center surface (cross section Q in Fig. 4 (a)). In the figure, the velocity of fluid in the back yoke room is comparatively larger which caused by the larger cross section and space. Fluid mixed flows obviously in both end regions, and the velocity distributions complex, and this would lead to an effective heat exchange for stator end windings.

The temperature distribution on the same cross section is shown in Fig. 6, in which the temperature belt clearly distributed. Although being droved by rotor, the heat transfer ability of moving air in air-gap is still very weak, so the heat will stayed longer time in rotor, thus highest temperature in motor appears at rotor, which is reach up to 236 ℃. Whereas for components at stator side, it will be directly cooled by the oil, and the temperature is relatively lower.
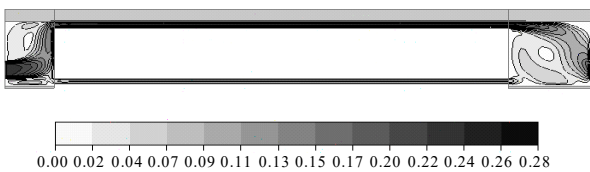
0.00 0.02 0.04 0.07 0.09 0.11 0.13 0.15 0.17 0.20 0.22 0.24 0.26 0.28
Fig. 5. Axial velocity distribution of cooling oil in HSPMG (in m/s).

operating		Measured			Calculated
Non-load cooling oil temperature	speed rpm	inlet	outlet	Temperature rise	Temperature rise
	21000	19.0	19.4	0.4	0.45
	36000	16.7	17.7	1.0	0.95
	48000	21.9	23.5	1.6	1.7

In this study, the basic experimental work is also processed. During the test, the flow rate of cooling oil is kept as 1.624m³/h. Form Table. II the coupling analyses results show good agreement with the measured data under different operating conditions.

In order to determine an optimized groove height, a groove height reduction coefficient is defined as the relative difference between the slot grooves outlet surface height h_2 and the inlet surface height h_1, that is dh=$(h_1-h_2)/h_1$. whist, the position variation coefficient is defined as dl= l_2/ l_1, (l_2 is the axial distance of the position where the slot groove cross section changes from the slot inlet surface, and the total groove length is l_1).

The influences of groove height variation (dh) and cross section changed positions (dl) on HSPMG temperature distributions are shown in Fig. 7. The change tendencies of the highest axial temperature (T_{max}) and the largest temperature difference (T_{det}) are similar. Due to their better axial thermal conductivity abilities, the T_{det} in the stator windings and rotor are much smaller than that in the stator core. While dl is between 0.48 and 0.60, the smallest T_{det} appears.

IV.   OPTIMIZATION FOR GROOVES STRUCTURE

In this investigation, both the highest working temperature T_{max} and the axial temperature difference T_{det} of HSPMG different components (stator windings, stator core, and rotor) are selected as the objective parameters for optimization. Taking the two parameters (dh and dl) as the variables, the slot cooling groove structure is optimized by using CQICO.

By using the linear weighted strategy, the multi-objective optimization problem is converted into a weighted summation function of all the optimization objectives, and the optimization model can be
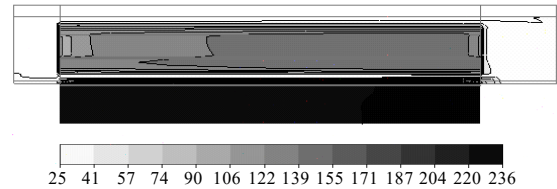
25 41 57 74 90 106 122 139 155 171 187 204 220 236
Fig. 6. Temperature distribution in solid region of analysis model.
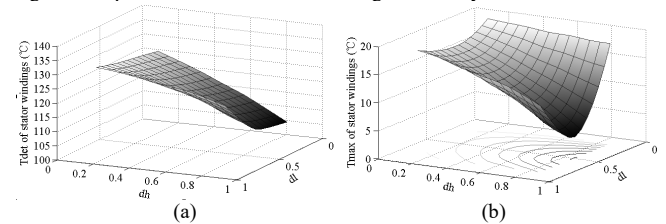
(a)   (b)
Fig. 7. Distributions of objective temperature: (a) the T_{max} of stator windings, (b) the T_{det} of stator windings.

$$\begin{cases} \min_{X \in D} F(X) = \min \sum_{i=1}^{k} \omega_i f_i(X), \quad X \in R^n \\ D = \left\{ X \middle| g_j(X) \le 0, \quad j = 1,2,\mathsf{L}, m \right\} \end{cases}, \quad (8)$$

where, $F(X) = [f_1(X), f_2(X), \cdots, f_6(X)]^T$, $X = [x_1, x_2]^T = [dh, dl]^T$. $f_1(X)$ is the T_{max} of stator windings, $f_2(X)$ is the T_{det} of stator windings, $f_3(X)$ is the T_{max} of stator core, $f_4(X)$ is the T_{det} of stator core, $f_5(X)$ is the T_{max} of rotor, $f_6(X)$ is the T_{det} of rotor, $g_i(X)$ is the convergence condition for optimized objectives. ω_i is the weighting factor, which satisfies $\sum^k \omega_i = 1$.

In the CQICO optimization, dh $\in$ [0.1428,0.8571], dl $\in$ [0.16,0.88], the antibody population size is 30, the mutation probability P_m=0.6, and the iterative evolutionary generation is set as 30. For the antibody i, in the k iteration, the objective function for cooling structure $F_i^k(X)$ is defined as the affinity G_i^k, that is

$$F_i^k(X) = G_i^k = \sum_{j=1}^{6} \omega_i f_{ji}^k(X_i^k) \cdot \quad (9)$$

Fig. 8 shows the evolutionary curves optimization with different algorithms, from which it can be seen that the same optimization results are obtained, and it needs just 6 iterations for CQICO to obtain the globally optimal solution, which is 16 times for ICO, and 29 times for GA(crossover probability P_c=0.78, and the mutation probability P_m=0.06). The optimal result is X=[0.8571, 0.5404]^T, and $F(X)$=[108.8258, 3.9902, 104.9708, 12.5672, 215.1999, 1.2906, 0.5404]^T, $\min \omega_i f_2(X)$ =71.6596.

Fig. 9 shows the comparisons of temperature distribution in HSPMG with different cooling grooves. Temperature in machine with new cooling grooves changes much smaller and distributes more evenly in the axial direction.

In Table. III, the objective temperatures determined by CQICO are close to those obtained from the numerical analyses. Cooled by the new groove, the T_{max} of the HSPMG stator windings reduces about 23.5 ℃, and it also reduces about 25.9 ℃ and 21.2 ℃ for stator core and rotor, respectively. Whilst, the axial temperature difference of stator windings to its highest temperature is reduced from 15% to
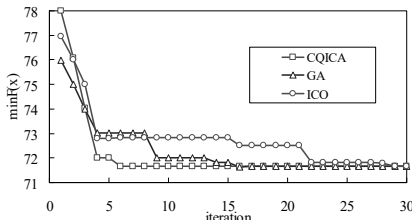
Fig. 8. Evolutionary curves of objective function.
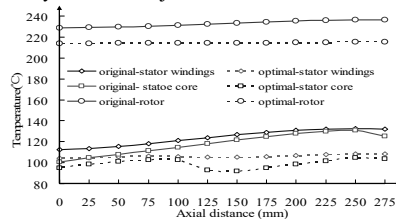
Fig. 9. Temperatures distributions in HSPMG with different grooves.

TABLE III
TEMPERATURES IN HSPMG WITH DIFFERENT STRUCTURES COOLING GROOVES (℃)

Positions	Original grooves		Optimal grooves			
			CQICO		Numerical analyses	
	T_{max}	T_{det}	T_{max}	T_{det}	T_{max}	T_{det}
Windings	132.32	19.87	108.83	3.99	108.85	4.06
Stator core	131.03	30.50	104.97	12.57	105.11	12.59
Rotor	236.36	7.56	215.20	1.29	215.14	1.31

3.7%, and it reduces from 3.2% to 0.6% for the rotor. Whereas for stator core, because of the poor heat transfer ability of lamination insulation in axial direction, its axial temperature difference is still comparatively larger, and the percentage is changed from 23.3% to 12.0%.

CONCLUSIONS

By using the coded qubits and quantum gates, the proposed novel CQICO has of better global searching capability and faster convergence. The optimized grooved structure for HSPMG obtained by the CQICO reduces the highest temperature and the axial temperature difference in machine different components up to 12%. It can be inferred that the new grooves structure with excellent effectiveness in bettering temperature distribution. However, in the practical utilizing, such a new structure would be limited by the groove size and the manufacture processing. The effectiveness of the groove structure is also influenced by the properties of cooling fluid.

REFERENCES

[1] L. Batista, F. G. J. Guimaraes, A. Ramirez, "A Distributed Clonal Selection Algorithm for Optimization in Electromagnetics". *IEEE Trans. on Magn.* 2009, vol. 45, no. 3, pp. 1598-1601.
[2] T.Hey, : "Quantum computing: An introduction". *Computing and Control Engineering Journal*, 1999, 10, (3), pp. 105–112.
[3] Licheng Jiao, Yangyang Li. "Quantum-Inspired Immune Clonal Optimization." *The 2005 IEEE International Conference on Neural Networks and Brain*, Beijing, China, 2005, 1, pp. 461 - 466.
[4] K.Watanabe, F. Campelo, Y. Iijima, *et. al.* "Optimization of inductors using evolutionary algorithms and its experimental validation". *IEEE Trans. on Magn.* 2010, vol. 46, no. 8, pp. 3393-3396.
[5] Vieira, D. A. G. A., Lisboa, C., Saldanha, R. R. : "An Enhanced Ellipsoid Method for Electromagnetic Devices Optimization and Design". *IEEE Trans. Magn.*, 2010, 46, (8), pp. 2843-2851.
[6] B. Zhang, A. Wang Li, Martin Doppelbauer. "Multi-Objective Optimization of a Transverse Flux Machine With Claw-Pole and Flux-Concentrating Structure", *IEEE Trans. Magn.* 2016, Vol. 52, No. 8, 8107410.
[7] Peter Gangl, Samuel Amstutz, Ulrich Langer. "Topology Optimization of Electric Motor Using Topological Derivative for Nonlinear Magnetostatics", *IEEE Trans. Magn.* 2016, Vol. 52, No. 3, 7201104.
[8] J. Buschbeck, M. Vogelsberger, A. Orellano, and Erich Schmidt . "Pareto Optimization in Terms of Electromagnetic and Thermal Characteristics of Air-Cooled Asynchronous Induction Machines Applied in Railway Traction Drives", *IEEE Trans. Magn.* 2016, Vol. 52, No. 3, 8101004.
[9] D. Gerada, A. Mebarki, N.L. Brown, et al. "Design Aspects of High-Speed High-Power-Density Laminated-Rotor Induction Machines", *IEEE Trans. Ind. Electron.*, vol. 58, no. 9, pp. 4039-4047, Sep. 2011.
[10] X. Zhang, W. Li, B. Kou, et al. "Electro-thermal combined optimization on notch in air cooled High Speed Permanent Magnetic Generator", *IEEE Trans. Magn.* 2015, Vol. 51, No. 1, 8200210.